CLNS 05-1926
CLEO 05-14

Observation of $\psi(3770) \to \pi\pi J/\psi$ and Measurement of $\Gamma_{ee}[\psi(2S)]$

N. E. Adam,[1] J. P. Alexander,[1] K. Berkelman,[1] D. G. Cassel,[1] V. Crede,[1] J. E. Duboscq,[1] K. M. Ecklund,[1] R. Ehrlich,[1] L. Fields,[1] R. S. Galik,[1] L. Gibbons,[1] B. Gittelman,[1] R. Gray,[1] S. W. Gray,[1] D. L. Hartill,[1] B. K. Heltsley,[1] D. Hertz,[1] C. D. Jones,[1] J. Kandaswamy,[1] D. L. Kreinick,[1] V. E. Kuznetsov,[1] H. Mahlke-Krüger,[1] T. O. Meyer,[1] P. U. E. Onyisi,[1] J. R. Patterson,[1] D. Peterson,[1] E. A. Phillips,[1] J. Pivarski,[1] D. Riley,[1] A. Ryd,[1] A. J. Sadoff,[1] H. Schwarthoff,[1] X. Shi,[1] M. R. Shepherd,[1] S. Stroiney,[1] W. M. Sun,[1] D. Urner,[1] T. Wilksen,[1] K. M. Weaver,[1] M. Weinberger,[1] S. B. Athar,[2] P. Avery,[2] L. Breva-Newell,[2] R. Patel,[2] V. Potlia,[2] H. Stoeck,[2] J. Yelton,[2] P. Rubin,[3] C. Cawlfield,[4] B. I. Eisenstein,[4] G. D. Gollin,[4] I. Karliner,[4] D. Kim,[4] N. Lowrey,[4] P. Naik,[4] C. Sedlack,[4] M. Selen,[4] E. J. White,[4] J. Williams,[4] J. Wiss,[4] D. M. Asner,[5] K. W. Edwards,[5] D. Besson,[6] T. K. Pedlar,[7] D. Cronin-Hennessy,[8] K. Y. Gao,[8] D. T. Gong,[8] J. Hietala,[8] Y. Kubota,[8] T. Klein,[8] B. W. Lang,[8] S. Z. Li,[8] R. Poling,[8] A. W. Scott,[8] A. Smith,[8] S. Dobbs,[9] Z. Metreveli,[9] K. K. Seth,[9] A. Tomaradze,[9] P. Zweber,[9] J. Ernst,[10] H. Severini,[11] S. A. Dytman,[12] W. Love,[12] S. Mehrabyan,[12] J. A. Mueller,[12] V. Savinov,[12] Z. Li,[13] A. Lopez,[13] H. Mendez,[13] J. Ramirez,[13] G. S. Huang,[14] D. H. Miller,[14] V. Pavlunin,[14] B. Sanghi,[14] I. P. J. Shipsey,[14] G. S. Adams,[15] M. Anderson,[15] J. P. Cummings,[15] I. Danko,[15] J. Napolitano,[15] Q. He,[16] H. Muramatsu,[16] C. S. Park,[16] E. H. Thorndike,[16] T. E. Coan,[17] Y. S. Gao,[17] F. Liu,[17] M. Artuso,[18] C. Boulahouache,[18] S. Blusk,[18] J. Butt,[18] O. Dorjkhaidav,[18] J. Li,[18] N. Menaa,[18] R. Mountain,[18] R. Nandakumar,[18] K. Randrianarivony,[18] R. Redjimi,[18] R. Sia,[18] T. Skwarnicki,[18] S. Stone,[18] J. C. Wang,[18] K. Zhang,[18] S. E. Csorna,[19] G. Bonvicini,[20] D. Cinabro,[20] M. Dubrovin,[20] R. A. Briere,[21] G. P. Chen,[21] J. Chen,[21] T. Ferguson,[21] G. Tatishvili,[21] H. Vogel,[21] M. E. Watkins,[21] and J. L. Rosner[22]

(CLEO Collaboration)

[1] *Cornell University, Ithaca, New York 14853*
[2] *University of Florida, Gainesville, Florida 32611*
[3] *George Mason University, Fairfax, Virginia 22030*
[4] *University of Illinois, Urbana-Champaign, Illinois 61801*
[5] *Carleton University, Ottawa, Ontario, Canada K1S 5B6*
[6] *University of Kansas, Lawrence, Kansas 66045*
[7] *Luther College, Decorah, Iowa 52101*
[8] *University of Minnesota, Minneapolis, Minnesota 55455*
[9] *Northwestern University, Evanston, Illinois 60208*
[10] *State University of New York at Albany, Albany, New York 12222*
[11] *University of Oklahoma, Norman, Oklahoma 73019*
[12] *University of Pittsburgh, Pittsburgh, Pennsylvania 15260*
[13] *University of Puerto Rico, Mayaguez, Puerto Rico 00681*
[14] *Purdue University, West Lafayette, Indiana 47907*
[15] *Rensselaer Polytechnic Institute, Troy, New York 12180*
[16] *University of Rochester, Rochester, New York 14627*
[17] *Southern Methodist University, Dallas, Texas 75275*

[18] *Syracuse University, Syracuse, New York 13244*
[19] *Vanderbilt University, Nashville, Tennessee 37235*
[20] *Wayne State University, Detroit, Michigan 48202*
[21] *Carnegie Mellon University, Pittsburgh, Pennsylvania 15213*
[22] *Enrico Fermi Institute, University of Chicago, Chicago, Illinois 60637*
(Dated: August 9, 2005)

Abstract

We observe signals for the decays $\psi(3770) \to XJ/\psi$ from data acquired with the CLEO detector operating at the CESR e^+e^- collider with $\sqrt{s}$=3773 MeV. We measure the following branching fractions $\mathcal{B}(\psi(3770) \to XJ/\psi)$ and significances: $(189 \pm 20 \pm 20) \times 10^{-5}$ (11.6σ) for $X = \pi^+\pi^-$, $(80 \pm 25 \pm 16) \times 10^{-5}$ (3.4σ) for $X = \pi^0\pi^0$, and $(87 \pm 33 \pm 22) \times 10^{-5}$ (3.5σ) for $X = \eta$, where the errors are statistical and systematic, respectively. The radiative return process $e^+e^- \to \gamma\psi(2S)$ populates the same event sample and is used to measure $\Gamma_{ee}[\psi(2S)] = (2.54 \pm 0.03 \pm 0.11)$ keV.

The $\psi(3770)$ charmonium state decays most copiously into $D\bar{D}$ pairs, but other decays similar to those of $\psi(2S)$ are predicted [1–8]. The $\psi(2S)$ mass eigenstate is expected [8] have a dominant $2\,^3S_1$ angular momentum eigenstate with a small 1^3D_1 admixture, and vice versa for the $\psi(3770)$. Because more than half of $\psi(2S)$ decays contain a J/ψ in the final state, a $2\,^3S_1$ component enhances similar transitions for $\psi(3770)$. Theoretical estimates [3, 5–7] of the rate for transitions from the $1\,^3D_1$ eigenstate, based on a QCD multipole expansion, span a broad range. BES reported the first sighting of a $\psi(3770)$ non-$D\bar{D}$ decay [9], at $\sim 3\sigma$ significance, with $\mathcal{B}(\psi(3770) \to \pi^+\pi^- J/\psi) = (0.34 \pm 0.14 \pm 0.09)\%$.

In this Letter we describe a search for the XJ/ψ final states, where $X = \pi^+\pi^-$, $\pi^0\pi^0$, η, and π^0, in e^+e^- collision data taken at a center-of-mass energy $\sqrt{s}$=3.773 GeV. We use $J/\psi \to \ell^+\ell^-$, where $\ell^\pm \equiv e^\pm$ or $\mu^\pm$. The data were acquired with the CLEO detector [10] operating at the Cornell Electron Storage Ring [11], and correspond to an integrated luminosity [12, 13] of $\mathcal{L} = (280.7 \pm 2.8)$ pb^{-1}. The process $e^+e^- \to \gamma\psi(2S)$ dominates this event sample and is treated as background; it also yields a measurement of $\Gamma_{ee}[\psi(2S)]$.

The primary background for $\psi(3770) \to XJ/\psi$ is the tail of the $\psi(2S)$ and radiative returns to it via initial state radiation (ISR) (*i.e.* $e^+e^- \to \gamma\psi(2S) \to \gamma XJ/\psi$); the total radiated energy peaks near 87 MeV but can take on a range of values. Similarly, there are radiative returns to that portion of the $\psi(3770)$ lineshape lying below $\sqrt{s}$ which constitute part of the signal. The differential cross section for $e^+e^- \to \gamma R \to \gamma XJ/\psi$, where $R = \psi(2S)$ or $\psi(3770)$, can be expressed [14–16] in terms of XJ/ψ mass-squared s' and the scaled radiated energy $x \equiv 1 - s'/s$ as

$$\frac{d\sigma}{dx} = W(s,x) \times b(s') \times F_X(s') \times \Gamma_{ee} \times \mathcal{B}_X \quad , \tag{1}$$

where $W(s,x)$ is the ISR γ-emission probability, $b(s')$ is the relativistic Breit-Wigner formula, $F_X(s')$ is the phase space factor [17] appropriate for X, Γ_{ee} is the e^+e^- partial width of R (including vacuum polarization effects), and $\mathcal{B}_X \equiv \mathcal{B}(R \to XJ/\psi)$ signifies an exclusive branching fraction. The ISR kernel is, at lowest order,

$$W(s, x > x_0) \equiv \frac{2\alpha}{\pi x}\left(\ln\frac{s}{m_e^2} - 1\right)\left(1 - x + \frac{x^2}{2}\right) , \tag{2}$$

in which $x_0 > 0$ is a cutoff to prevent the divergence of $\int W\,dx$, m_e is the electron mass, and α is the fine structure constant. The Breit-Wigner function is

$$b(s) \equiv \frac{12\pi\Gamma_R}{(s - M_R^2)^2 + M_R^2\Gamma_R^2} , \tag{3}$$

in which Γ_R is the full width and M_R the nominal mass. The phase space factor is $F_X(s') \equiv (p_X/p_0)^{2L+1}$, in which p_X is the momentum of X in the R center-of-mass frame, p_0 is the value of p_X at $\sqrt{s'} = M_R$, and L is the relative orbital angular momentum between X and J/ψ. Eq. (1) has one enhancement near $x = 0$ due to the $1/x$ factor in $W(s,x)$, and, for s sufficiently larger than M_R^2, a much larger one near $x = 1 - M_R^2/s$, corresponding to the peak of the Breit-Wigner resonance function.

The cross section $\sigma(s)$ for $e^+e^- \to \gamma R \to \gamma XJ/\psi$ can be both obtained from Eq. (1) and measured:

$$\sigma(s) = \frac{N}{\epsilon \times \mathcal{L}} = \Gamma_{ee} \times \mathcal{B}_X \times I(s) , \tag{4}$$

in which N is the number of events counted and ϵ is the detection efficiency obtained from Monte Carlo (MC) simulation, and the integral

$$I(s) \equiv \int W(s,x) b(s') F_X(s')\, dx \tag{5}$$

is insensitive to the value of Γ. Hence a measurement of $\sigma(s)$ for $R = \psi(2S)$ can be combined with $\mathcal{B}_X$ measurements [18] to yield $\Gamma_{ee}[\psi(2S)]$.

We choose the E_γ cutoff to be 2 MeV ($x_0 = 1.06 \times 10^{-3}$), small enough that events with $x < x_0$ are experimentally indistinguishable from those with $x = x_0$. The expression [14–16] for $W(s, x < x_0)$ includes terms accounting for soft and virtual photon emission (but not vacuum polarization, which is included in Γ_{ee}); we obtain $I(s, x < x_0) = 0.62\, b(s)\, F_X(s)$, a result reproduced by the Babayaga [13] $\mu^+\mu^-$ event generator. The integral $I(s, x > x_0)$ can be performed numerically. For $W(s, x > x_0)$, we employ the full expression including higher order radiative corrections as given in Eq. (28) of Ref. [14]; it gives values $\sim$19% smaller than Eq. (2) for J/ψ radiative returns from $\sqrt{s} = 3.773$ GeV.

The `EvtGen` event generator [19], which includes final state radiation [20], and a GEANT-based [21] detector simulation are used to model the physics processes. The generator implements a relative S-wave (P-wave) configuration between the $\pi\pi$ (η or π^0) and the J/ψ. Radiative returns to $\psi(2S)$ and $\psi(3770)$ for $x > x_0$ are generated with the polar angle distribution from Refs. [16], and account for ISR according to Eqs. (1-3). Separately, XJ/ψ events are also generated without a photon to represent all $x < x_0$ events from $\psi(2S)$ and $\psi(3770)$, and are weighted with respect to the $x > x_0$ events according to the $I(s, x < x_0)/I(s, x > x_0)$ ratios.

Event selection implements the same requirements as in the CLEO $\psi(2S) \to XJ/\psi$ analysis [18] except for the changes described here. No X-recoil mass cuts are imposed. To increase acceptance for $J/\psi \to \ell^+\ell^-$, lepton candidates at small polar angles ($0.85 < |\cos\theta_\ell| < 0.93$) are added. A number of measures are taken to reduce backgrounds. We demand $m(\ell^+\ell^-) = 3.05 - 3.14$ GeV, and add to each lepton momentum vector any photon candidates located within a 100 mrad cone of the initial lepton direction. All π^0 candidates must satisfy $m(\gamma\gamma) =$ 110-150 MeV. For $X = \pi^+\pi^-$, neither pion candidate can be identified as an electron if $m(\pi^+\pi^-) < 450$ MeV, which suppresses $e^+e^- \to \ell^+\ell^-\gamma$, $\gamma \to e^+e^-$ events in which the e^+e^- pair from the photon conversion is mistaken for the $\pi^+\pi^-$. For $X = \pi^+\pi^-$ and $\pi^0\pi^0$, we require $m(\pi\pi) > 350$ MeV. For the $\pi^0 J/\psi(\to e^+e^-)$ and $\eta(\to \gamma\gamma) J/\psi(\to e^+e^-)$ modes, background from Bhabha events is diminished by requiring $\cos\theta_{e^+} < 0.3$. For $X = \pi^0$ or $\eta(\to \gamma\gamma)$, radiative transitions from $\psi(3770)$ or the $\psi(2S)$ tail to χ_{cJ} are suppressed by requiring the least energetic photon in the π^0 or η candidate to satisfy $E_\gamma > 280$ MeV or $E_\gamma =$ 30-170 MeV.

To extract the number of $\psi(2S)$ and $\psi(3770)$ events, we fit the distribution of event missing momentum, which can be interpreted as a measure of E_γ,

$$k = \frac{s - M_J^2 + m_X^2 - 2\sqrt{s\,(p_X^2 + m_X^2)}}{2\left(\sqrt{p_J^2 + M_J^2} - p_J \cos\phi\right)}\ , \tag{6}$$

in which M_J is the nominal J/ψ mass, p_J is the measured dilepton momentum, p_X is the measured X momentum, m_X is the mass of X (the PDG value [22] for $X = \eta, \pi^0$, or the measured mass for $X = \pi\pi$), and ϕ is the measured angle between the J/ψ and the event missing momentum three-vector ($\mathbf{k}$). The small ($\sim$2 mrad) crossing angle of the incoming $e^{\pm}$ beams has been neglected.

The phase space [17] factor for $F_{\pi\pi}(s')$ is not as simple as the $(p_X/p_0)^3$ dependence for η and π^0 because the $\pi\pi$ mass varies. The average momentum of the $\pi\pi$ system increases by $\sim$11% from $\sqrt{s'}$=3.686 GeV to 3.773 GeV. As the $\pi\pi$ and J/ψ are in a relative S-wave, we set $F_{\pi\pi}(s'=(3.773 \text{ GeV})^2)$=1.11; for other s', $F_{\pi\pi}$ is scaled linearly with x. The functional form of $F_{\pi\pi}$ is not crucial because $d\sigma/dx$ is small over the central portion of the interval $E_\gamma = 0$-87 MeV.

The distribution in k for each exclusive mode is subjected to a maximum likelihood fit for three components with floating normalizations: a radiative return to $\psi(2S)$ shape obtained from MC simulation, a direct decay $\psi(3770) \to XJ/\psi$ signal shape from MC simulation (including radiative returns to the $\psi(3770)$ tail), and a background component linear in k. Direct decays from the $\psi(3770)$ and the tail of the $\psi(2S)$ add incoherently [6], so that the $\psi(2S)$ background can be included without regard for interference.

The distributions and fits are shown in Figs. 1-3. The fit results and quantities derived from them appear in Table I. The efficiencies include the MC correction factors from Ref. [18], the visible cross sections use $\mathcal{B}(J/\psi \to \ell^+\ell^-)$ from Ref. [23], and the Γ_{ee} values use the $\mathcal{B}(\psi(2S) \to XJ/\psi)$ results from Ref. [18]. Statistical significances of the $\psi(3770)$ signals, obtained from the differences in log-likelihoods between fits with and without a signal component, are shown, indicating an unambiguous $\pi^+\pi^-J/\psi$ signal, and suggestive $\pi^0\pi^0J/\psi$ and $\eta J/\psi$ signals. The product of the measured cross section $\sigma(D\bar{D})$ [24] and luminosity $\mathcal{L}$ is used to give the number of produced $\psi(3770)$ decays as $(1.80\pm0.03^{+0.04}_{-0.02})\times10^6$. Sidebands around $M(J/\psi)$ in the dilepton mass distributions for events near the radiative return peak in k do not show evidence for additional background. Feed-across background (from radiative returns to $\psi(2S)$ but with non-signal $\psi(2S)$ decays) levels and uncertainties are determined using measured branching fractions [18] and MC simulation, as in Ref. [18].

The results for $\gamma\psi(2S) \to \gamma\pi^0J/\psi$ are all treated as upper limits due to substantial backgrounds from radiative Bhabha and muon pair events. Efficiency-corrected, background-subtracted rates for $J/\psi \to e^+e^-$ and $J/\psi \to \mu^+\mu^-$ are consistent with each other. Allowing second or third order polynomials in the background parameterizations has a negligible effect upon Γ_{ee}.

Statistical errors dominate for the $\psi(3770)$ results and systematic errors dominate for the $\psi(2S)$ results. Table II summarizes the uncertainties that are uncorrelated for different X. The systematic errors on the fitted event yields include changes induced by variation of the range in k of the fit and the alternate use of a χ^2 fit instead of maximum likelihood. The efficiency uncertainties are larger than in Ref. [18] because here the leptons are not restricted to $|\cos\theta_\ell| < 0.83$, the $\pi^0 \to \gamma\gamma$ and $J/\psi \to \ell^+\ell^-$ mass cuts are tighter, and we account for imperfections in the assumed $\psi(2S)$ boost direction.

Relative uncertainties that are correlated for all X include those from $\mathcal{B}(J/\psi \to \ell^+\ell^-)$ (0.94% statistical, 0.71% systematic), $I(s)$ (*i.e.* radiative corrections) (2.0%), $\mathcal{L}$ (1.0%), and the normalization portion of $\mathcal{B}_X$ (3.0%). The MC sample used for this analysis has a mean and spread of $\sqrt{s}$ very close to that of the data, within 0.05 MeV and 0.02 MeV, respectively, rendering negligible any remaining systematic effect upon $I(s)$.

A single value, $\Gamma_{ee}[\psi(2S)] = (2.54\pm0.03\pm0.11)$ keV, is obtained by combining $\pi^+\pi^-J/\psi$, $\pi^0\pi^0J/\psi$, and $\eta J/\psi$ results, weighting each by the uncorrelated statistical and systematic errors. The relative 4.4% total uncertainty is dominated by the common 3.0% systematic normalization uncertainty in all CLEO $\psi(2S)$ branching fraction measurements [18]. It is 2.5 standard deviations higher than and of comparable precision to the PDG fit value, (2.12 ± 0.12) keV [22]; it is within two standard deviations of any of the results obtained from scanning the $\psi(2S)$ peak, the most precise of which is the preliminary BES [25] result, $(2.25 \pm 0.11 \pm 0.02)$ keV.

Figure 4 shows the $m(\pi^+\pi^-)$ and ℓ^+ polar angle distributions for $\pi^+\pi^- J/\psi$ events restricted to $k = [-10, +10]$ MeV, background-subtracted with the sum of the $[-57, -17]$ and $[+13, +53]$ MeV sidebands scaled down by a factor of four. The MC histograms are normalized to the same areas as the data. In both plots, neither data nor MC is corrected for detection efficiency. The data points represent events from both $\psi(3770)$ and $\psi(2S)$ in a ratio of ∼2:1. The measured $m(\pi^+\pi^-)$ and $|\cos\theta(\ell^+)|$ distributions show consistency with the $\psi(2S)$-like S-wave MC predictions.

The branching fraction for $\psi(3770) \to \pi^+\pi^- J/\psi$ is smaller than that reported by BES [9], but is consistent with it and more precise. While the widths for $\psi(3770) \to \pi\pi J/\psi$ are in the broad range predicted by the QCD multipole expansion models [2, 3, 6, 7], the $\pi\pi$ mass distribution appears to be much stiffer than predicted for the large D-wave proportion featured in these models. The branching fraction for $\psi(3770) \to \pi\pi J/\psi$ also relates to the interpretation of the $X(3872)$: the small value does not strengthen the case for conventional charmonium [26]. The results combine to give $\Sigma_X \mathcal{B}(\psi(3770) \to X J/\psi) = (0.36 \pm 0.06)\%$, which corresponds to a cross section of (23 ± 5) pb. The 90% C.L. upper limits are $\mathcal{B}(\psi(3770) \to \eta J/\psi,\ \pi^0 J/\psi) < 0.15\%,\ 0.028\%$; substantially more data would be required to quantitatively probe the $c\bar{c}$ purity of the $\psi(2S)$ and $\psi(3770)$ as proposed in Ref. [27].

In summary, we have observed the first statistically compelling signal for non-$D\bar{D}$ decays of the $\psi(3770)$, and with the same data sample have achieved improved precision on $\Gamma_{ee}[\psi(2S)]$.

We gratefully acknowledge the effort of the CESR staff in providing us with excellent luminosity and running conditions. This work was supported by the National Science Foundation and the U.S. Department of Energy.

[1] N. Brambilla *et al.*, hep-ph/0412158 (2004) (unpublished).
[2] T.M. Yan, Phys. Rev. D **22**, 1652 (1980).
[3] Y.P. Kuang and T.M. Yan, Phys. Rev. D **24**, 2874 (1981).
[4] H.J. Lipkin, Phys. Lett. **B179**, 278 (1986).
[5] K. Lane, Harvard Report No. HUTP-86/A045 (1986) (unpublished).
[6] Y.P. Kuang and T.M. Yan, Phys. Rev. D **41**, 155 (1990).
[7] Y.P. Kuang, Phys. Rev. D **65**, 094024 (2002).
[8] J.L. Rosner, Phys. Rev. D **64**, 094002 (2001).
[9] J.Z. Bai *et al.* (BES Collaboration), Phys. Lett. **B605**, 63 (2005).
[10] Y. Kubota *et al.* (CLEO Collaboration), Nucl. Instrum. Methods Phys. Res., Sect. A **320**, 66 (1992); D. Peterson *et al.*, Nucl. Instrum. Methods Phys. Res., Sect. A **478**, 142 (2002); M. Artuso *et al.*, Nucl. Instrum. Methods Phys. Res., Sect. A **502**, 91 (2003).
[11] R.A. Briere *et al.* (CLEO-c/CESR-c Taskforces and CLEO-c Collaboration), Cornell LEPP Report No. CLNS 01/1742, 2001 (unpublished).
[12] G. Crawford *et al.* (CLEO Collaboration), Nucl. Instrum. Methods Phys. Res., Sect. A **345**, 429 (1994).
[13] C.M. Carloni Calame *et al.*, Nucl. Phys. Proc. Suppl. B **131**, 48 (2004).
[14] E.A. Kuraev and V.S. Fadin, Sov. J. Nucl. Phys. **41**, 466 (1985);
[15] J.P. Alexander *et al.*, Nucl. Phys. **B320**, 45 (1989).
[16] G. Bonneau and F. Martin, Nucl. Phys. **B27**, 381 (1971); M. Benayoun *et al.*, Mod. Phys. Lett. **A14**, 2605 (1999).
[17] J.D. Jackson, Nuovo Cimento **34**, 1644 (1964); S.U. Chung *et al.* (E852 Collaboration), Phys. Rev. D **60**, 092001 (1999).
[18] N.E. Adam *et al.* (CLEO Collaboration), Phys. Rev. Lett. **94**, 232002 (2005).
[19] D.J. Lange, Nucl. Instrum. Methods Phys. Res., Sect. A **462**, 152 (2001).
[20] E. Barberio and Z. Was, Comput. Phys. Commun. **79**, 291 (1994).
[21] R. Brun *et al.*, GEANT 3.21, CERN Program Library Long Writeup W5013 (1993), unpublished.
[22] S. Eidelman *et al.*, Phys. Lett. **B592**, 1 (2004).
[23] Z. Li *et al.* (CLEO Collaboration), Phys. Rev. D **71**, 111103 (2005).
[24] Q. He *et al.* (CLEO Collaboration), Phys. Rev. Lett. **95**, 121801 (2005).
[25] M. Ablikim *et al.* (BES Collaboration), Contributed paper LP2005-452 at the *XXII International Symposium on Lepton-Photon Interactions at High Energy, Uppsala, Sweden, June 30-July 5, 2005* (unpublished).
[26] T. Barnes and S. Godfrey, Phys. Rev. D **69**, 054008 (2004); E.J. Eichten, K. Lane, and C. Quigg, Phys. Rev. D **69**, 094019 (2004).
[27] M.B. Voloshin, Phys. Rev. D **71**, 114003 (2005).

TABLE I: Results for radiative return process $e^+e^- \to \gamma\psi(2S)$, $\psi(2S) \to XJ/\psi$ and direct decay $\psi(3770) \to XJ/\psi$. For each appears the fit yield N, efficiency ϵ, and cross section σ. In addition, for the radiative return process, the integral $I(s)$ [followed by its value for $x < x_0$], and the $\mathcal{B}(\psi(2S) \to XJ/\psi) \times \Gamma_{ee}$ values inferred from σ appear along with the resulting Γ_{ee}. The bottom five rows include the significance in standard deviations of the $\psi(3770) \to XJ/\psi$ signals and the $\psi(3770)$ branching fraction and partial width. Errors shown are statistical and systematic, respectively.

X	$\pi^+\pi^-$	$\pi^0\pi^0$	η	π^0
$N(\gamma\psi(2S) \to \gamma XJ/\psi)$	$19469 \pm 145 \pm 195$	$3616 \pm 64 \pm 72$	$291 \pm 19 \pm 15$	< 37
$\epsilon(\gamma\psi(2S) \to \gamma XJ/\psi)$ (%)	$56.23 \pm 0.07 \pm 0.90$	$21.66 \pm 0.06 \pm 0.65$	$7.89 \pm 0.17 \pm 0.28$	$11.33 \pm 0.12 \pm 0.66$
$\sigma(\gamma\psi(2S) \to \gamma XJ/\psi)$ (pb)	$1036 \pm 13 \pm 23$	$500 \pm 10 \pm 19$	$111 \pm 8 \pm 8$	< 10
$I(s)$ (pb/keV)	1215.4 [6.7]	1215.4 [6.7]	1251.9 [34.2]	1215.2 [8.9]
$\mathcal{B}(\psi(2S) \to XJ/\psi) \times \Gamma_{ee}$ (eV)	$852 \pm 10 \pm 26$	$411 \pm 8 \pm 18$	$88 \pm 6 \pm 7$	< 8
$\Gamma_{ee}[\psi(2S)]$ (eV)	$2541 \pm 32 \pm 113$	$2488 \pm 54 \pm 138$	$2716 \pm 191 \pm 217$	$< 6.2 \times 10^3$
$N(\psi(3770) \to XJ/\psi)$	$231 \pm 24 \pm 23$	$39 \pm 12 \pm 8$	$22 \pm 8 \pm 6$	< 10 @90% C.L.
Significance	11.6σ	3.4σ	3.5σ	0σ
$\epsilon(\psi(3770) \to XJ/\psi)$ (%)	$57.05 \pm 0.16 \pm 0.91$	$22.86 \pm 0.13 \pm 0.69$	$11.80 \pm 0.13 \pm 0.43$	$16.02 \pm 0.15 \pm 0.93$
$\sigma(\psi(3770) \to XJ/\psi)$ (pb)	$12.1 \pm 1.8 \pm 1.2$	$5.1 \pm 2.0 \pm 1.0$	$5.5 \pm 2.1 \pm 1.4$	< 1.8 @90% C.L.
$\mathcal{B}(\psi(3770) \to XJ/\psi)$ (10^{-5})	$189 \pm 20 \pm 20$	$80 \pm 25 \pm 16$	$87 \pm 33 \pm 22$	< 28 @90% C.L.
$\Gamma(\psi(3770) \to XJ/\psi)$ (keV)	$45 \pm 5 \pm 7$	$19 \pm 6 \pm 4$	$21 \pm 8 \pm 6$	< 7 @90% C.L.

TABLE II: Uncorrelated relative uncertainties in percent for the results in Table I; for correlated errors, see text.

X	$\pi^+\pi^-$	$\pi^0\pi^0$	η	π^0
$\psi(2S)$ yield (stat)	0.7	1.8	6.5	19
$\psi(3770)$ yield (stat)	10	31	36	–
$\psi(2S)$ yield (sys)	1.0	2.0	5.0	10
$\psi(3770)$ yield (sys)	10	20	25	–
Efficiency	1.6	3.0	3.6	5.8
$\psi(2S)$ Feed-across	0.1	0.1	3.0	50
$\mathcal{B}(\psi(2S) \to XJ/\psi)$ stat	0.4	0.9	1.9	7.7
$\mathcal{B}(\psi(2S) \to XJ/\psi)$ sys	1.3	1.8	1.6	7.1

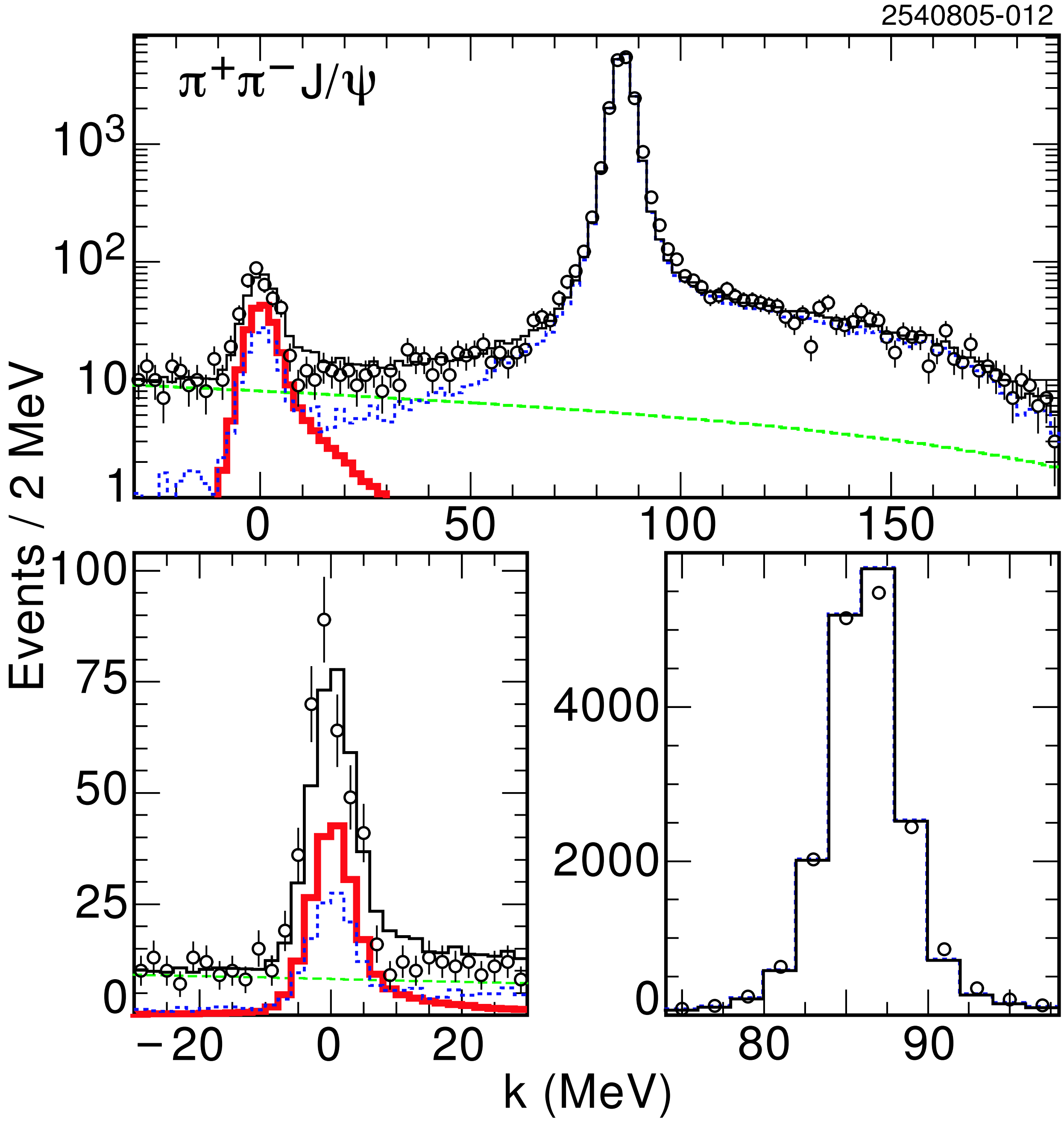

FIG. 1: Fit of the distribution in k for the final state $\pi^+\pi^- J/\psi$, showing the data (open circles), overall fit (thin solid line), direct $\psi(3770)$ decay peak (thick solid line), radiative return to the $\psi(2S)$ (dotted line), and the background term (dashed line), on a logarithmic vertical scale (top), and on linear vertical scales focussed on the direct decay peak (bottom left) and radiative return peak (bottom right).

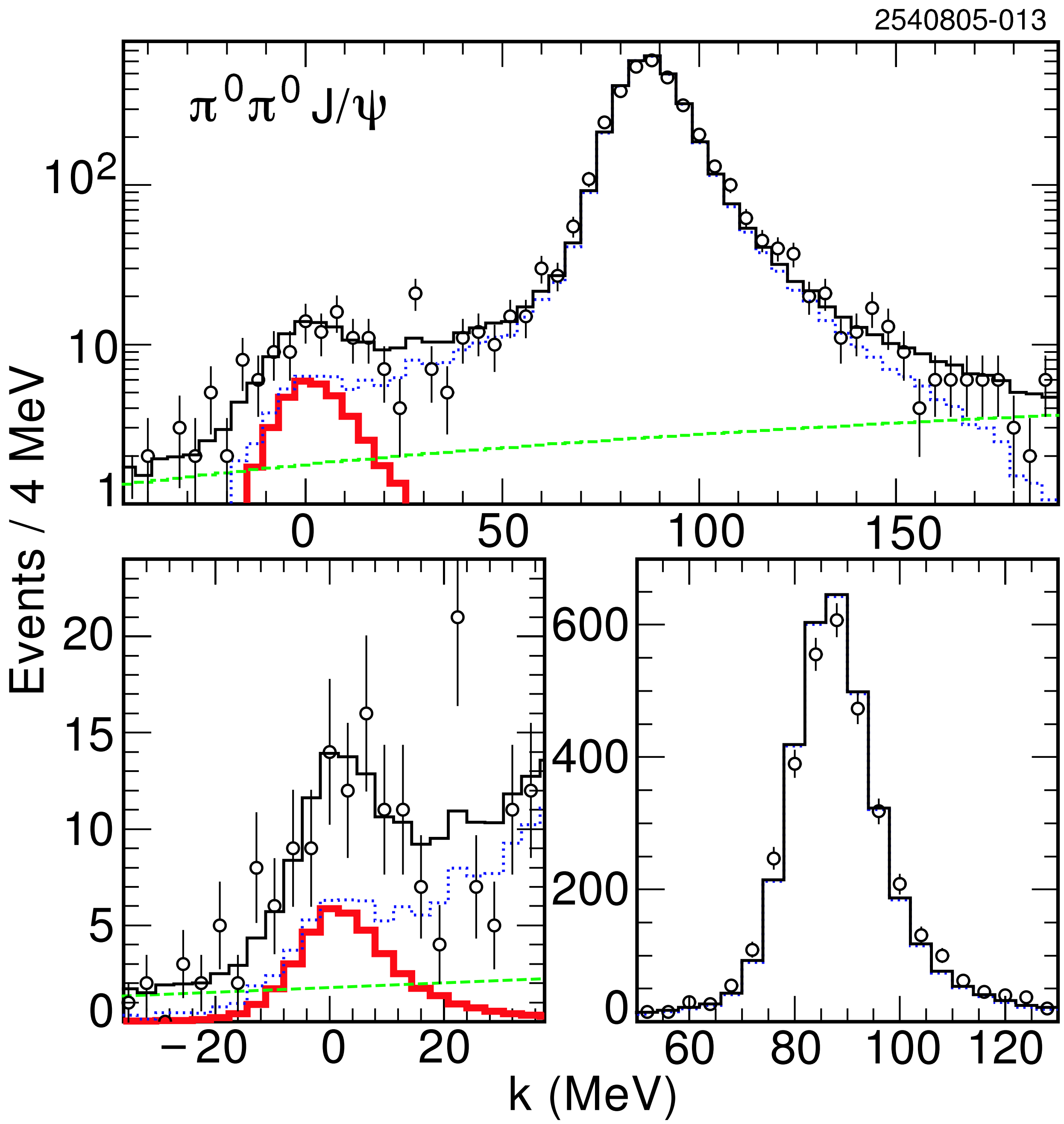

FIG. 2: Fit of the distribution in k for the final state $\pi^0\pi^0 J/\psi$, showing the data (open circles), overall fit (thin solid line), direct $\psi(3770)$ decay peak (thick solid line), radiative return to the $\psi(2S)$ (dotted line), and the background term (dashed line), on a logarithmic vertical scale (top), and on linear vertical scales focussed on the direct decay peak (bottom left) and radiative return peak (bottom right).

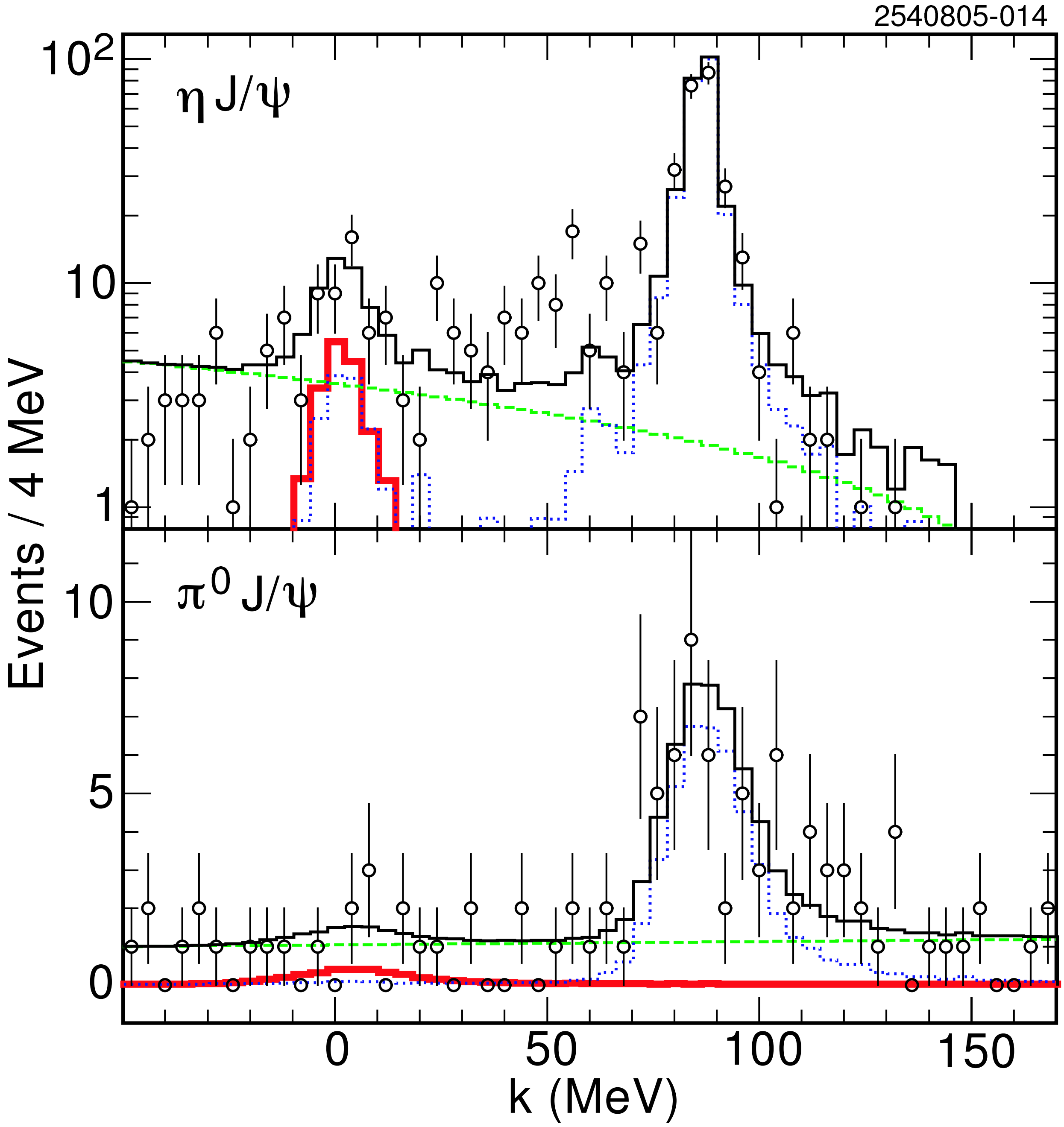

FIG. 3: Fit of the distribution in k for the final state $\eta J/\psi$ (top) and $\pi^0 J/\psi$ (bottom), showing for each the data (open circles), overall fit (thin line), direct $\psi(3770)$ decay peak (thick solid line), radiative return to the $\psi(2S)$ (dotted line), and the background term (dashed line).

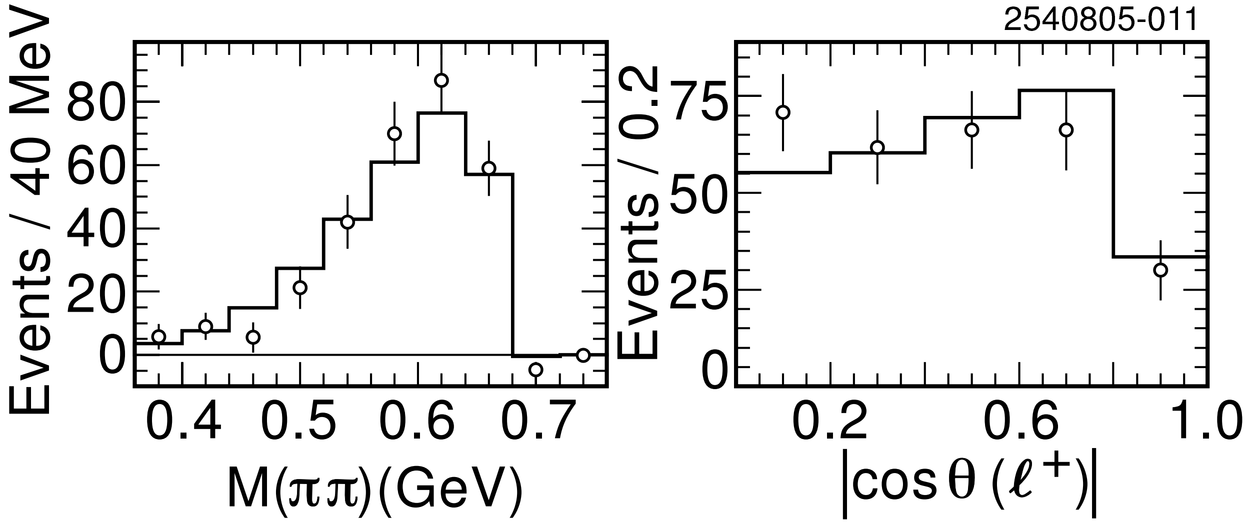

FIG. 4: Distributions in $\pi^+\pi^-\ell^+\ell^-$ events of the $\pi^+\pi^-$ mass (left) and polar angle (right) of the positively charged lepton from data (open circles) and MC (solid line line).